water

MDPI

Communication

Land–Sea Distribution of Ground Precipitation in Mediterranean Storms

Renzo Rosso and Alessandro Ceppi *

Department of Civil and Environmental Engineering (DICA), Politecnico di Milano, Piazza Leonardo da Vinci 32, 20133 Milan, Italy

* Correspondence: alessandro.ceppi@polimi.it

Abstract: The Mediterranean basin is traditionally a hotspot where copious amounts of water vapor at low- and mid-tropospheric levels often favor atmospheric instability and the deepening of storms, leading to intense rainfall events with consequent flash floods. Moreover, this region includes sharp land–sea transitions, narrow maritime areas, and mountain chains which enhance convective precipitation. In this study, radar precipitation data were used to investigate the spatial distribution of rainfall swaths for seven severe cyclones originating over the Mediterranean Sea which produced intense flash inundation events along the western coast of Italy in the last decade (2011–2020). Based on 5 min precipitation amounts gridded at a 1 km spatial resolution, the temporal evolution of these storms displays a curvilinear path moving from sea to inland. Results show that more than half of the total precipitation for the analyzed events occurred on sea, and the total amount of storm rainfall over the marine surface exceeded that over land in four events out of the seven. Since the coastline strongly affects the rainfall pattern, we analyzed the land–sea discontinuity, which is a key factor controlling the spatial distribution of storm rates through their trajectory, where a small shift in precipitation target might smooth ground effects and mitigate flood impacts.

Keywords: Mediterranean storms; flash floods; radar analysis; land–sea precipitation; rainfall swaths

Citation: Rosso, R.; Ceppi, A. Land–Sea Distribution of Ground Precipitation in Mediterranean Storms. *Water* **2023**, *15*, 1894. https://doi.org/10.3390/w15101894

Academic Editors: Roberto Coscarelli and Tommaso Caloiero

Received: 18 March 2023
Revised: 5 May 2023
Accepted: 10 May 2023
Published: 17 May 2023

1. Introduction

The Mediterranean basin is the core of a highly active atmospheric circulation area because of its location in the transition zone between the subtropical high-pressure belt and the mid-latitude westerlies [1,2] with distinctly different properties of air masses. The frequency, duration, and intensity of cyclonic circulations play a crucial role in weather and climate over the entire region [3], whose disturbances have a heavy ground effect able to trigger flash floods in coastal areas [4–9]. However, the link between the intensity of these cyclones and hazardous extreme events is not always linear, and various characteristics can be involved as different impacts are considered [10].

Studies about cyclones in the Mediterranean region have been carried out since the second half of the 20th century [11] until today [12]. Starting from the last decade of the previous century, appropriate techniques were introduced to identify and track the genesis and evolution of these Mediterranean low-pressure systems, and to provide a deeper insight into the dynamics and temporal variability of their cyclogenesis [13–20]. In the last twenty years, research studies have primarily addressed the modeling and observational aspects of Mediterranean cyclones, such as the MEDEX [21] and the HyMeX [22] projects, while further analyses examined the connections of these storms and climate change, since the Mediterranean is considered a particularly vulnerable area [23–27].

The Mediterranean is a relatively small region, but with a unique and complex geography. It is characterized by a nearly enclosed basin with sharp land–sea transitions and prominent mountain chains surrounding it. Climatological studies showed that Mediterranean cyclogenesis is clearly modulated by orography [28–31]. In particular, the Italian

regions Liguria and Tuscany, where six out of the seven events analyzed in this paper were located, are often affected by severe floods due to their position, exposed to southerly moist flows from the Mediterranean Sea and steep slopes near the coasts [32–37].

Severe storms occur every year over the Mediterranean basin, particularly during a negative NAO phase [38]. Regarding the seasonal cycle, extreme precipitation is usually observed between late summer and mid-autumn, when heat and moisture fluxes from the Mediterranean Sea are the highest, suggesting a fundamental role of sea surface temperature (SST) in the generation and evolution of convective systems and subsequent floods [39]. According to the Mediterranean Flood Fatalities (MEFF) database and its extended version, the EUFF (European Flood Fatalities), covering the 1980–2018 period [40,41], the flood-related mortality due to Mediterranean storms mainly occurs during early autumn in the western Mediterranean area, and during late autumn and winter in the eastern Mediterranean. This is basically in accordance with the investigated events in this study over the western coast of Italy, among which the most severe ones are included, and which occurred in the autumn seasons between the years 2011 and 2017, where the damages due to the collapse of bridges, roads, and levees as well as landslides, debris flows, and inundations were estimated at billions of EUR (Euros), with many fatalities, unfortunately, in each of the analyzed events.

The aim of this study is to evaluate the spatialized patterns of storm formation areas in the Mediterranean Sea, where most flash flood disasters occur in a narrow strip a few kilometers from the coast. This paper is, hence, structured as follows: Section 2 deals with the adopted methodology of radar image acquisition for the seven analyzed events, Section 3 illustrates the main outcomes of the research about the pattern of spatial rainfall distribution over land and sea, while Section 4 shows a simulation scenario performed under the assumption that the land precipitation volume was shifted offshore and, therefore, slightly reduced with a consequent massive mitigation of ground impacts.

2. Methodology

In this section, the adopted methodology about the rainfall radar image acquisition for each of the analyzed events is described. The following procedure pursues our objective to analyze the relative amount of total precipitation over sea and coastal land during these severe storms. Seven extreme episodes occurred along the western coast of north–central Italy from 2011 to 2017: these major cyclones were selected based on the severity of impacts, i.e., causalities and damages, and they are reported in Table 1.

Unfortunately, at the time of the examined flash flood events (extreme in terms of ground effects), the Italian radar network was not fully operating. Instead, a complete and available dataset was obtained from the Meteo France radar located in Aleria town, on the east coast of the Corsica region, which is in front of the central–west coast of Italy with no orographic obstacles present towards the direction of the Italian seashores; hence, this S-band radar with an operational range of about 300 km was chosen to for the radar imagery for the specific area where flash floods occurred.

Accordingly, the Direction des Services Meteorologiques of the Meteo France administration delivered the preprocessed gridded radar images in order to provide the accumulated 5 min precipitation with a 1 km resolution. For further information about the quantitative precipitation estimates (QPE) provided by Meteo France, the reader can refer to Figueras and Tabary [42] for a complete review about the French operational radar rainfall product.

Digital image processing was conducted with an algorithm which automatically identifies the area of interest (different from one event to another) for every image. Consequently, the algorithm performs the rainfall swaths from pixel information to a temporal sequence of maps to determine the storm trajectory. The region of interest (ROI) is contoured to consider the main storm direction, and it has a different shape for each event: an example of the ROI is indicated in Figure 1.

Table 1. List of investigated storms. The source of information is from local Italian media and press.

#	Location	Date	Death Toll	Details
1	Cinque Terre	25 October 2011	13	About EUR 200 million of damage, as well as irreversible injury to the local landscape, recorded in this site of the UNESCO World Heritage List. More than 1100 evacuees.
2	Elba	7 November 2011	1	High level of damage to roads, bridges, and municipal infrastructures: EUR 3 million costs to face emergency in Elba Island. Many landslides and debris flows.
3	Maremma	12 November 2012	6	Both rivers and canals overflowed the banks and inundated residential, commercial, and industrial areas. More than 700 evacuees.
4	Massa Carrara	12 November 2012	1	Overflowing of some creeks inundated urban areas. Water depth up to 1 m for several days. Many landslides. Total of 5000 buildings damaged and more than 300 evacuees. Power blackout and municipal water supply stoppage.
5	Sardinia (Olbia)	18 November 2013	18	Several bridges collapsed, roads interrupted, inaccessibility of many country villages. Large agricultural areas flooded.
6	Orbetello	14 October 2014	2	Maximum warning level by National Civil Protection. Heavy damage to bridges, roads, and levees caused the inundation of a large agricultural area in the countryside.
7	Livorno	9 September 2017	8	Maximum warning level by National Civil Protection. Overflowing of a small creek caused the inundation of a large urban area.

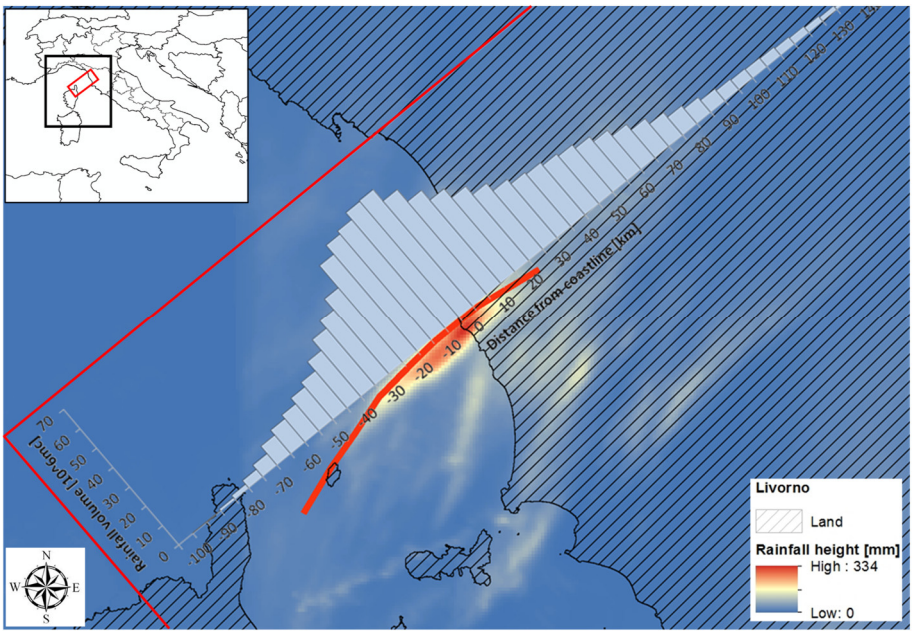

Figure 1. Example of the ROI (red rectangles) for the Livorno event, where the spatial distribution path of precipitation swaths is shown with a red line. In the upper left box, the geographical area of Italy is shown; in particular, the black square depicts the Mediterranean region where the seven analyzed events occurred.

Once the ROI was selected, the algorithm discriminated between land and sea regions, and it subdivided the "no-land" territory in progressive distance bands from the coastline, considering an interval of 1 km for each band. The image acquisition processed all pictures which composed the event, summing the precipitation values in each band. The final information was the total rainfall for each progressive distance along the considered main

direction and for each event every 5 min. The methodology can be summarized in the following flow chart (Figure 2):

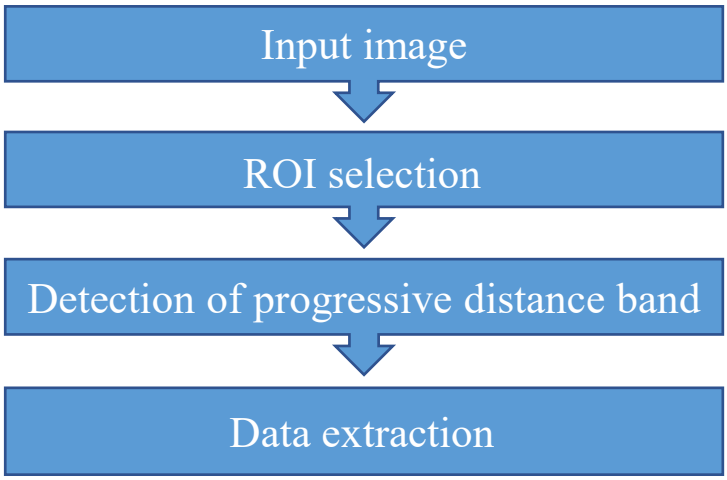

Figure 2. Flow chart of the adopted methodology for the image acquisition.

From the radar image analysis, rainfall data were extracted considering the 5 min precipitation amounts along the main trajectory of the storm. For each event, the time integral of precipitation depth was estimated as in Equation (1):

$$H(s) = \int_{\tau} h(t,s)dt \quad (1)$$

This provides a detailed spatial distribution pattern of rainfall over sea and land. Therefore, taking into account the total event duration [τ] and summing the rainfall value [h] for each time [t], the spatial distribution of total rainfall [$H(s)$] can be obtained.

3. Results

Since the analysis aims to investigate the spatial evolution of the cyclones, the sea–coastline trajectories were examined, focusing on the variation in precipitation rate throughout the main storm directions. The total hyetographs in Figure 3 show that the maximum rainfall value occurred in the proximity of the coastline for the events in Livorno, Elba, Cinque Terre, Maremma, and Sardinia (Olbia), and in a 50 km span from the coastline for the other two events, Massa Carrara and Orbetello.

The results point out that the coastline strongly affects the rainfall pattern. This discontinuity is one of the major factors controlling the spatial distribution of the storm rates throughout their trajectory. In most cases, the maximum total rainfall occurred in the proximity of the coastline before making landfall. Furthermore, it is interesting to investigate the amount of rainfall over land and sea areas. Figure 4 depicts the percentage of sea (y axis) and land (x axis) precipitation for each analyzed event. In three episodes out of the seven (Elba, Sardinia, and Massa Carrara), there was a significant percentage (above 60%) of precipitation over the sea surface, while in another three events (Maremma, Cinque Terre, and Livorno), the land–sea distribution was close to 50%; only the Orbetello case, in which the rainfall peak was totally located inland, shows a value of over 90% land precipitation.

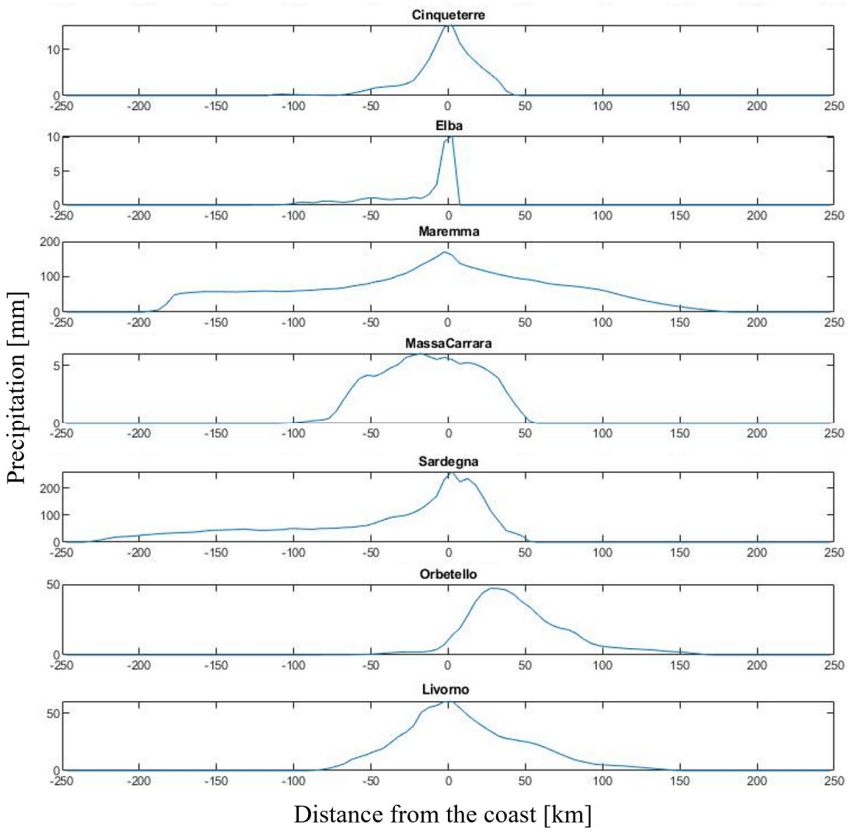

Figure 3. Total hyetographs of the seven events in regard to the distance from the coast. Positive distances are on land, while negatives are on sea.

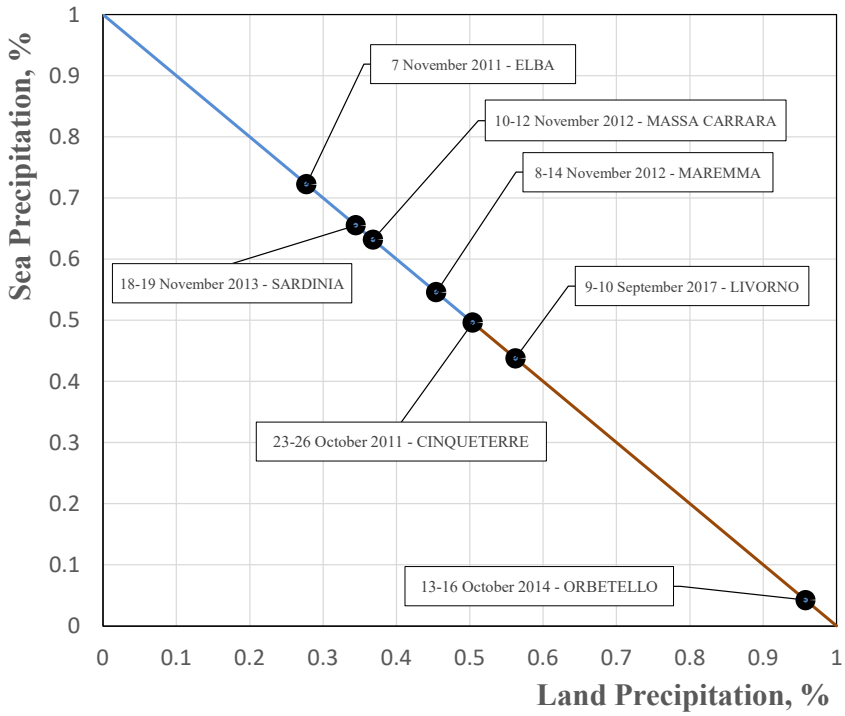

Figure 4. Percentage of rainfall over land and sea for each considered event. Colors on the main diagonal line depict where most of the precipitation fell in each event: blue over sea and brown over land.

4. Discussion

To highlight the importance of the coastal transition and to quantify the ground effect of the sea–land precipitation ratio, the Elba flood case was examined in detail. Figure 5 shows the inundated area in the village Marina di Campo, a coastal area (5.7 km^2) downstream of the Fosso degli Alzi creek.

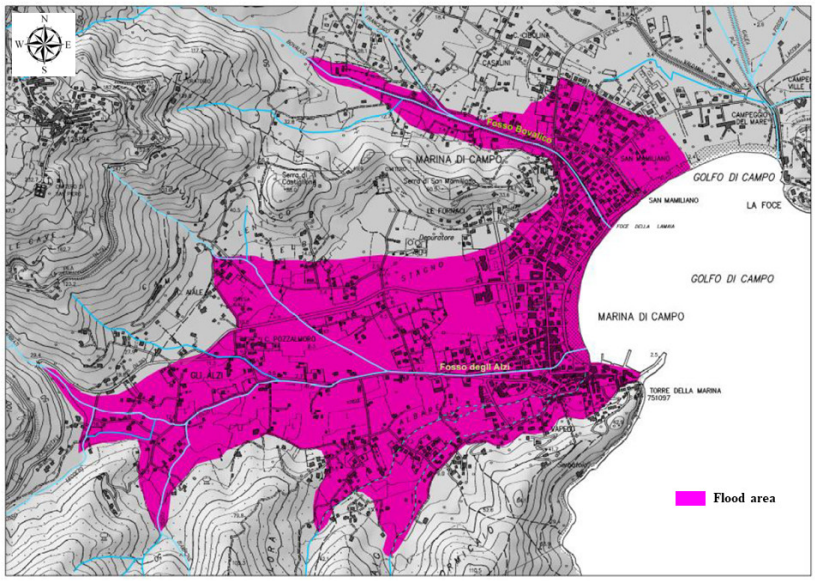

Figure 5. The inundated zone (in fuchsia), downstream of the coastal area of the Fosso degli Alzi creek on 7 November 2011, reconstructed by merging field investigations of the rescue squad immediately after the event with satellite data.

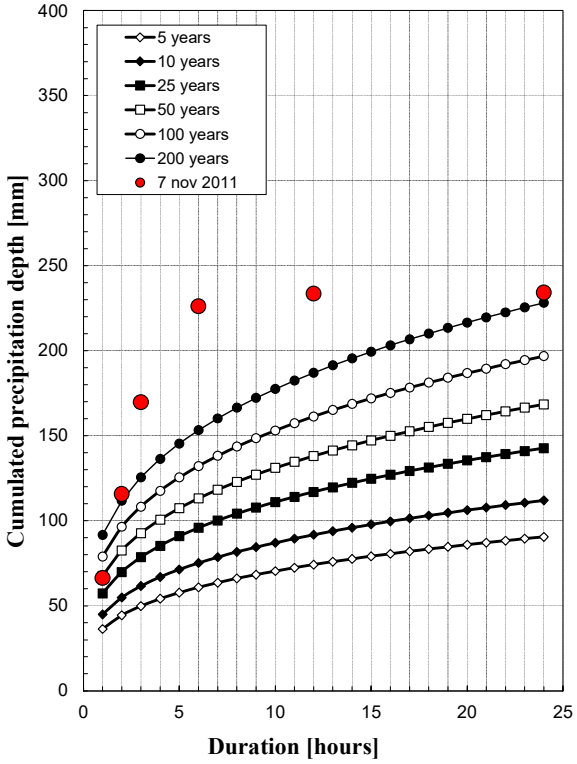

Figure 6. Comparison of maximum precipitation totals for different durations with the depth–duration–frequency curves at Marina di Campo, estimated from simple scaling using the General Extreme Value distribution [43].

Comparing the storm event data with the current depth–duration–frequency curves, estimates of this precipitation event largely exceeded the 200-year return period in the range from 3 to 12 h (Figure 6). It is significant to underline how the storm produced erosion, and the transportation of ancient debris (including gravel, pebbles, and impressive boulders) in the upstream area of iron mines, once exploited by the Roman empire, abandoned there centuries ago.

From a hydrological point of view, the flood hydrograph was reconstructed using a simple model which couples the SCS-CN (Soil Conservation Service–Curve Number) method, currently used in Italy for flood frequency estimation [44] with the Gamma Instantaneous Unit Hydrograph (IUH) parametrized using the Horton Order Ratios [45], with the lag time estimated from field observations during and after the disaster. From the analysis of radar records, it was deduced that 27.7 percent of this total storm precipitation was land rainfall, while the remaining (72.3 percent) was over sea.

Afterwards, a further simulation scenario was performed under the assumption that the land precipitation volume was reduced from 27.7 to 22.2 percent of the total by moving an extra 5.5 percent of rainfall offshore. The land impacts of this exercise are truly amazing, because the flood peak would decrease by about 20 percent: from about 100 m^3/s to 80 m^3/s (see Figure 7). Therefore, even a very small shift in the precipitation target [46] could drastically smooth ground effects and mitigate flood impacts, an issue which might become relevant from the perspective of climate change scenarios and coastal flood vulnerability [47–51].

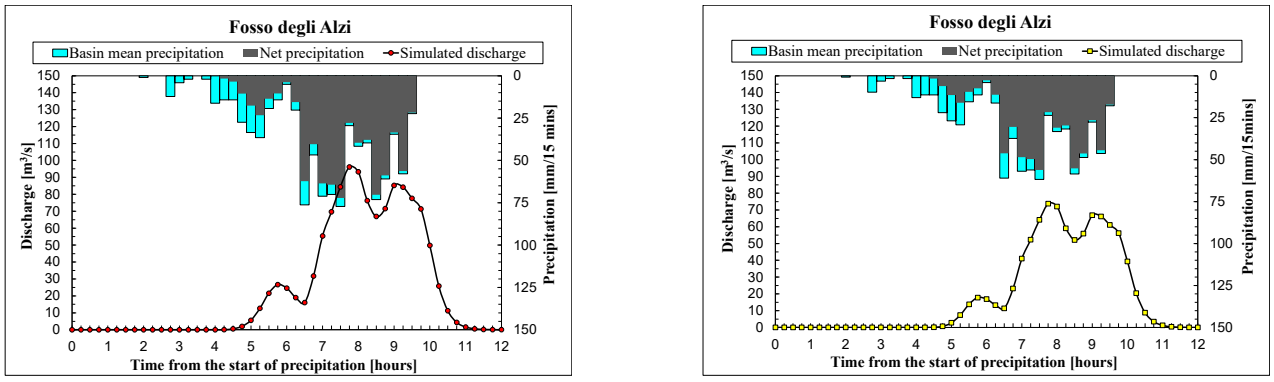

Figure 7. Discharge reconstruction for the observed Elba event with a land–sea precipitation ratio of 0.277 (**a**), and for a simulated scenario of the same event with a ratio of 0.222 (**b**).

5. Conclusions

The present study shows the land–sea distribution of ground precipitation in Mediterranean storms for seven events in the western coast of north–central Italy, where large numbers of damaged infrastructures and casualties occurred between 2011 and 2017. These types of storms always constitute a major threat in the Mediterranean region as they are associated with intense winds, abundant-to-extreme rainfall, and flooding, with impacts on coastal areas [52].

In this paper, each event was investigated through the available imagery database made available by the Meteo France service to analyze the spatial distribution of precipitation. This study evaluated the land–sea percentage of ground precipitation observed for each event. Except for the Orbetello case, where the precipitation was totally inland, the others measured distributed rainfall over sea surface values greater than or equal to 50%. This issue underlines the importance of the land–sea precipitation ratio, since a slight precipitation shift towards or away from inland may dramatically change the flood hydrograph of the river basin, with consequent smoothing (or enhancing) of ground impacts. Therefore, since the spatial distribution and trajectory of Mediterranean cyclones are strictly correlated with possible destruction of territory, future developments into these specific

aspects can be useful for predicting and better understanding the interaction between these Mediterranean storms and the land–sea discontinuity over the coastal territory.

Finally, we pose ourselves a provocative question about active meteorological controls: if future efforts are fostered in the direction of producing small and controlled modifications of storm precipitation over coastal areas, could the mitigation of floods be improved with consequence reduction in their severity and impacts due to the non-linearity of the basin response? For decades, human attempts in weather manipulation have been ineffective, and we are aware even now that different methods are used without achieving scientifically consistent results. Nevertheless, recent studies [53–55] astonishingly found that the presence of offshore wind farms can inadvertently alter land precipitation patterns, even causing a statistically significant reduction in downstream and onshore rainfall due to changes in horizontal wind divergence and in vertical velocity. This may be an open challenge for the next decades.

Author Contributions: R.R.: Conceptualization, Investigation, Resources, Writing—review and editing, Funding acquisition, Supervision. A.C.: Formal analysis, Investigation, Data curation, Methodology, Writing—original draft, Writing—review and editing. All authors have read and agreed to the published version of the manuscript.

Funding: This work has been supported by Fondazione Cariplo, grant 2017-0708, "FLORIMAP—smart FLOod RIsk MAnagement Policies".

Data Availability Statement: Data will be made available on request.

Acknowledgments: Andrea Soncini and Cristina Deidda are gratefully acknowledged for their computational support.

Conflicts of Interest: The authors declare that they have no known competing financial interests or personal relationships that could have appeared to influence the work reported in this paper.

References

1. Ulbrich, U.; Leckebusch, G.C.; Pinto, J.G. Extra-tropical cyclones in the present and future climate: A review. *Theor. Appl. Climatol.* **2009**, *96*, 117–131. [CrossRef]
2. Neu, U.; Akperov, M.G.; Bellenbaum, N.; Benestad, R.; Blender, R.; Caballero, R.; Wernli, H. IMILAST: A community effort to intercompare extratropical cyclone detection and tracking algorithms. *Bull. Am. Meteorol. Soc.* **2013**, *94*, 529–547. [CrossRef]
3. Radinovic, D. *Mediterranean Cyclones and Their Influence on the Weather and Climate*; PSMP Report Ser. No. 24; WMO: Geneva, Switzerland, 1987; p. 131.
4. Jansa, A.; Genovés, A.; Garcia-Moya, J.A. Western Mediterranean cyclones and heavy rain. Part 1: Numerical experiment concerning the Piedmont flood case. *Meteorol. Appl.* **2000**, *7*, 323–333. [CrossRef]
5. De Zolt, S.; Lionello, P.; Nuhu, A.; Tomasin, A. The disastrous storm of 4 November 1966 on Italy. *Nat. Hazards Earth Syst. Sci.* **2006**, *6*, 861–879. [CrossRef]
6. Lionello, P.; Cavaleri, L.; Nissen, K.M.; Pino, C.; Raicich, F.; Ulbrich, U. Severe marine storms in the Northern Adriatic: Characteristics and trends. *Phys. Chem. Earth Parts A/B/C* **2012**, *40*, 93–105. [CrossRef]
7. Pfahl, S.; Wernli, H. Quantifying the relevance of cyclones for precipitation extremes. *J. Clim.* **2012**, *25*, 6770–6780. [CrossRef]
8. Terranova, O.G.; Gariano, S.L. Rainstorms able to induce flash floods in a Mediterranean-climate region (Calabria, southern Italy). *Nat. Hazards Earth Syst. Sci.* **2014**, *14*, 2423–2434. [CrossRef]
9. Amengual, A.; Borga, M.; Ravazzani, G.; Crema, S. The role of storm movement in controlling flash flood response: An analysis of the 28 September 2012 extreme event in Murcia, southeastern Spain. *J. Hydrometeorol.* **2021**, *22*, 2379–2392. [CrossRef]
10. Lionello, P.; Bhend, J.; Buzzi, A.; Della-Marta, P.M.; Krichak, S.O.; Jansà, A.; Maheras, P.; Sanna, A.; Trigo, I.F.; Trigo, R. Chapter 6 Cyclones in the Mediterranean region: Climatology and effects on the environment. In *Mediterranean Climate Variability*; Elsevier: Amsterdam, The Netherlands, 2006; Volume 4, pp. 325–372. [CrossRef]
11. Petterssen, S. *Weather Analysis and Forecasting*; Mac Graw Hill: New York, NY, USA, 1956; Volume 1, 428p.
12. Flaounas, E.; Davolio, S.; Raveh-Rubin, S.; Pantillon, F.; Miglietta, M.M.; Gaertner, M.A.; Hatzaki, M.; Homar, V.; Khodayar, S.; Korres, G.; et al. Mediterranean cyclones: Current knowledge and open questions on dynamics, prediction, climatology and impacts. *Weather Clim. Dyn.* **2022**, *3*, 173–208. [CrossRef]
13. Buzzi, A.; Tosi, E. Statistical behavior of transient eddies near mountains and implications for theories of lee cyclogenesis. *J. Atmos. Sci.* **1989**, *46*, 1233–1249. [CrossRef]
14. Tosi, E.; Buzzi, A. Characteristics of high-frequency atmospheric eddies over the Mediterranean area in different seasons. *Il Nuovo Cim. C* **1989**, *12*, 439–452. [CrossRef]

15. Alpert, P.; Neeman, B.U.; Shay-El, Y. Climatological analysis of Mediterranean cyclones using ECMWF data. *Tellus* **1990**, *42*, 65–77. [CrossRef]
16. Trigo, I.F.; Davies, T.D.; Bigg, G.R. Objective climatology of cyclones in the Mediterranean region. *J. Clim.* **1999**, *12*, 1685–1696. [CrossRef]
17. Campins, J.; Genoves, A.; Jansa, A.; Guijarro, J.A.; Ramis, C. A catalogue and a classification of surface cyclones for the western Mediterranean. *Int. J. Climatol.* **2000**, *20*, 969–984. [CrossRef]
18. Maheras, P.; Flocas, H.A.; Patrikas, I.; Anagnostopoulou, C. A 40-year objective analysis of surface cyclones in the Mediterranean region: Spatial and temporal distribution. *Int. J. Climatol.* **2001**, *21*, 109–130. [CrossRef]
19. Maheras, P.; Flocas, H.; Anagnostopoulou, C.; Patrikas, I. On the vertical structure of composite surface cyclones in the Mediterranean region. *Theor. Appl. Climatol.* **2002**, *71*, 199–217. [CrossRef]
20. Jansa, A.; Genoves, A.; Picornell, M.A.; Campins, J.; Riosalido, R.; Carretero, O. Western Mediterranean cyclones and heavy rain, Part 2: Statistical approach. *Meteorol. Appl.* **2001**, *8*, 43–56. [CrossRef]
21. Jansa, A.; Alpert, P.; Arbogast, P.; Buzzi, A.; Ivančan-Picek, B.; Kotroni, V.; Llasat, M.C.; Ramis, C.; Richard, E.; Romero, R.; et al. MEDEX: A general overview. *Nat. Hazards Earth Syst. Sci.* **2014**, *14*, 1965–1984. [CrossRef]
22. Drobinski, P.; Ducrocq, V.; Alpert, P.; Anagnostou, E.; Béranger, K.; Borga, M.; Braud, I.; Chanzy, A.; Davolio, S.; Delrieu, G.; et al. HyMeX: A 10-year multidisciplinary program on the Mediterranean water cycle. *Bull. Am. Meteorol. Soc.* **2014**, *95*, 1063–1082. [CrossRef]
23. Lionello, P.; Dalan, F.; Elvini, E. Cyclones in the Mediterranean region: The present and the doubled CO_2 climate scenarios. *Clim. Res.* **2002**, *22*, 147–159. [CrossRef]
24. Bengtsson, L.; Hodges, K.I.; Roeckner, E. Storm Tracks and Climate Change. *J. Clim.* **2006**, *19*, 3518–3543. [CrossRef]
25. Lionello, P.; Giorgi, F. Winter precipitation and cyclones in the Mediterranean region: Future climate scenarios in a regional simulation. *Adv. Geosci.* **2007**, *12*, 153–158. [CrossRef]
26. Raible, C.C.; Ziv, B.; Saaroni, H.; Wild, M. Winter synoptic scale variability over the Mediterranean Basin under future climate conditions as simulated by the ECHAM5. *Clim. Dyn.* **2010**, *35*, 473–488. [CrossRef]
27. Reale, M.; Cabos, W.; Cavicchia, L.; Conte, D.; Coppola, E.; Flaounas, E.; Giorgi, F.; Gualdi, S.; Hochman, A.; Li, L.; et al. Future projections of Mediterranean cyclone characteristics using the Med-CORDEX ensemble of coupled regional climate system models. *Clim. Dyn.* **2021**, *58*, 2501–2524. [CrossRef]
28. Campins, J.; Genovés, A.; Picornell, M.; Jansa, A. Climatology of Mediterranean cyclones using the ERA-40 dataset. *Int. J. Climatol.* **2011**, *31*, 1596–1614. [CrossRef]
29. Messmer, M.; Gómez-Navarro, J.J.; Raible, C.C. Climatology of Vb cyclones, physical mechanisms and their impact on extreme precipitation over Central Europe. *Earth Syst. Dyn.* **2015**, *6*, 541–553. [CrossRef]
30. Hofstätter, M.; Chimani, B.; Lexer, A.; Blöschl, G. A new classification scheme of European cyclone tracks with relevance to precipitation. *Water Resour. Res.* **2016**, *52*, 7086–7104. [CrossRef]
31. Lionello, P.; Trigo, I.F.; Gil, V.; Liberato, M.L.R.; Nissen, K.M.; Pinto, J.G.; Raible, C.C.; Reale, M.; Tanzarella, A.; Trigo, R.M.; et al. Objective climatology of cyclones in the Mediterranean region: A consensus view among methods with different system identification and tracking criteria. *Tellus A* **2016**, *68*, 29391. [CrossRef]
32. Silvestro, F.; Gabellani, S.; Giannoni, F.; Parodi, A.; Rebora, N.; Rudari, R.; Siccardi, F. A hydrological analysis of the 4 November 2011 event in Genoa. *Nat. Hazards Earth Syst. Sci.* **2012**, *12*, 2743–2752. [CrossRef]
33. Silvestro, F.; Rebora, N.; Giannoni, F.; Cavallo, A.; Ferraris, L. The flash flood of the Bisagno Creek on 9th October 2014: An unfortunate combination of spatial and temporal scales. *J. Hydrol.* **2015**, *541*, 50–62. [CrossRef]
34. Rebora, N.; Molini, L.; Casella, E.; Comellas, A.; Fiori, E.; Pignone, F.; Siccardi, F.; Silvestro, F.; Tanelli, S.; Parodi, A. Extreme rainfall in the Mediterranean: What can we learn from observations? *J. Hydrometeorol.* **2013**, *14*, 906–922. [CrossRef]
35. Buzzi, A.; Davolio, S.; Malguzzi, P.; Drofa, O.; Mastrangelo, D. Heavy rainfall episodes over Liguria of autumn 2011: Numerical forecasting experiments. *Nat. Hazards Earth Syst. Sci.* **2014**, *14*, 1325–1340. [CrossRef]
36. Cassola, F.; Ferrari, F.; Mazzino, A. Numerical simulations of Mediterranean heavy precipitation events with the WRF model: A verification exercise using different approaches. *Atmos. Res.* **2015**, *164–165*, 210–225. [CrossRef]
37. Faccini, F.; Luino, F.; Paliaga, G.; Roccati, A.; Turconi, L. Flash Flood Events along the West Mediterranean Coasts: Inundations of Urbanized Areas Conditioned by Anthropic Impacts. *Land* **2021**, *10*, 620. [CrossRef]
38. Nissen, K.M.; Leckebusch, G.C.; Pinto, J.G.; Renggli, D.; Ulbrich, S.; Ulbrich, U. Cyclones causing wind storms in the Mediterranean: Characteristics, trends and links to large-scale patterns. *Nat. Hazards Earth Syst. Sci.* **2010**, *10*, 1379–1391. [CrossRef]
39. Gaume, E.; Borga, M.; Llasat, M.C.; Maouche, S.; Lang, M.; Diakakis, M. Mediterranean extreme floods and flash floods. In *The Mediterranean Region under Climate Change: A Scientific Update*; Moatti, J.-P., Thiébault, S., Eds.; Allenvi: Marseille, France; IRD Editions: Marseille, France, 2016; Chapter 1.3.4; pp. 133–144.
40. Vinet, F.; Bigot, V.; Petrucci, O.; Papagiannaki, K.; Llasat, M.C.; Kotroni, V.; Boissier, L.; Aceto, L.; Grimalt, M.; Llasat-Botija, M.; et al. Mapping Flood-Related Mortality in the Mediterranean Basin. Results from the MEFF v2.0 DB. *Water* **2019**, *11*, 2196. [CrossRef]
41. Petrucci, O.; Papagiannaki, K.; Aceto, L.; Boissier, L.; Kotroni, V.; Grimalt, M.; Llasat, M.C.; Llasat-Botija, M.; Rosselló, J.; Pasqua, A.A.; et al. MEFF: The database of Mediterranean Flood fatalities (1980 to 2015). *J. Flood Risk Manag.* **2019**, *12*, e12461. [CrossRef]

42. Figueras, J.; Tabary, P. The new French operational polarimetric radar rainfall rate product. *J. Appl. Meteorol. Climatol.* **2013**, *52*, 1817–1835. [CrossRef]
43. De Michele, C.; Kottegoda, N.T.; Rosso, R. IDAF curves of extreme storm rainfall: A scaling approach. *Water Sci. Technol.* **2002**, *45*, 83–90. [CrossRef]
44. Bocchiola, D.; Rosso, R. Use of a derived distribution approach for flood prediction in poorly gauged basins: A case study in Italy. *Adv. Water Resour.* **2009**, *32*, 1284–1296. [CrossRef]
45. Rosso, R. Nash model relation to Horton order ratios. *Water Resour. Res.* **1984**, *20*, 914–920. [CrossRef]
46. Lombardi, G.; Ceppi, A.; Ravazzani, G.; Davolio, S.; Mancini, M. From Deterministic to Probabilistic Forecasts: The 'Shift-Target' Approach in the Milan Urban Area (Northern Italy). *Geosciences* **2018**, *8*, 181. [CrossRef]
47. Trenberth, K.E. Changes in precipitation with climate change. *Climento Res.* **2011**, *47*, 123–138. [CrossRef]
48. Balica, S.F.; Wright, N.G.; van der Meulen, F. A Flood Vulnerability Index for Coastal Cities and Its Use in Assessing Climate Change Impacts. *Nat. Hazards* **2012**, *64*, 73–105. [CrossRef]
49. Alfieri, L.; Burek, P.; Feyen, L.; Forzieri, G. Global warming increases the frequency of river floods in Europe. *Hydrol. Earth Syst. Sci.* **2015**, *19*, 2247–2260. [CrossRef]
50. Feng, X.; Liu, C.; Xie, F.; Lu, J.; Chiu, L.S.; Tintera, G.; Chen, B. Precipitation characteristic changes due to global warming in a high-resolution (16 km) ECMWF simulation. *Q. J. R. Meteorol. Soc.* **2019**, *145*, 303–317. [CrossRef]
51. IPCC. Climate Change 2022: Impacts, Adaptation, and Vulnerability. Available online: https://www.ipcc.ch/report/ar6/wg2/ (accessed on 15 February 2023).
52. Martzikos, N.T.; Prinos, P.E.; Memos, C.D.; Tsoukala, V.K. Statistical analysis of Mediterranean coastal storms. *Oceanologia* **2021**, *63*, 133–148. [CrossRef]
53. Fiedler, B.; Bukovsky, M. The effect of a giant wind farm on precipitation in a regional climate model. *Environ. Res. Lett.* **2011**, *6*, 045101. [CrossRef]
54. Pan, Y.; Yan, C.; Archer, C.L. Precipitation reduction during Hurricane Harvey with simulated offshore wind farms. *Environ. Res. Lett.* **2018**, *13*, 084007. [CrossRef]
55. Al Fahel, N.; Archer, C.L. Observed onshore precipitation changes after the installation of offshore wind farms. *Bull. Atmos. Sci. Technol.* **2020**, *1*, 179–203. [CrossRef]